Available online at www.sciencedirect.com
SCIENCE DIRECT®
Bioorganic & Medicinal Chemistry 13 (2005) 3987–3992
Bioorganic & Medicinal Chemistry

Theoretical study revealing the functioning of a novel combination of catalytic motifs in histone deacetylase

K. Vanommeslaeghe,[a,b,*] F. De Proft,[a] S. Loverix,[a,c] D. Tourwé[b] and P. Geerlings[a]

[a]*Vrije Universiteit Brussel, General Chemistry Group, Pleinlaan 2, B-1050 Brussel, Belgium*
[b]*Vrije Universiteit Brussel, Organic Chemistry Group ORGC, Pleinlaan 2, B-1050 Brussel, Belgium*
[c]*Vlaams Interuniversitair Instituut voor Biotechnologie, Department of Molecular and Cellular Interactions, Pleinlaan 2, B-1050 Brussel, Belgium*

Received 4 March 2005; accepted 1 April 2005
Available online 5 May 2005

Abstract—Histone deacetylases (HDACs) have recently attracted considerable interest as targets in the treatment of cell proliferative diseases such as cancer. In the present work, the chemical properties of the active site of HDAC were theoretically investigated at a high computational level. Evidence was gathered for a novel catalytic mechanism, which differs from a previous proposal in the native protonation state of the His–Asp dyads, and in the deprotonation of water as a distinct step in the mechanism.

1. Introduction

Histone deacetylases (HDACs) are very promising targets for so-called mechanism-based anti-cancer drugs that may combine clinical efficacy with relatively mild toxicological side effects.[1,2] Medicinal applications of HDAC inhibitors are however not limited to the treatment of cancer, but may vary from fibrotic diseases,[3] including liver fibrosis,[4,5] an important cause of death in Western society, over autoimmune[6] and inflammatory[7] diseases, to polyglutamin disease.[8,9] Also, they have been shown to inhibit dedifferentiation in cell cultures.[5] Not only do histone deacetylases regulate chromatin structure, recent discoveries indicate that the histone deacetylase isoform HDAC6 actually functions as a tubulin deacetylase and plays a major role in tubulin remodelling events, which are vital for mitosis.[10]

Since the HDAC family appears to play a key role in a very diverse set of regulatory events in the cell,[11] understanding its common reaction mechanism may yield valuable information for drug development. The X-ray structure of HDLP (histone deacetylase like protein, an HDAC analogue with the same active site as any member of the HDAC family), was, until very recently, the only available structure that provides information in this respect.[12] After completion of the present work, X-ray structures of inhibitor-bound human HDAC8, another HDAC isoform, were published by two independent groups,[13,14] showing that the catalytic site is essentially the same as in HDLP (see 'Discussion'). However, the precise catalytic mechanism of these enzymes still remains unclear, as the active site exhibits features of both serine proteases and zinc proteases. Moreover, they contain two adjacent His–Asp dyads, unlike any other enzymes known to us. In line of the current tendencies towards the application of quantum chemical methods to biosystems and its successes,[15–19] a DFT study on this system is presented, on the basis of which a proposal was made regarding the catalytic mechanism of the HDAC family (Scheme 1).

2. Computational details

2.1. Energy minimisations

Gaussian 03 was used for all calculations.[20] DFT energy minimisations were performed using the basis set and degrees of freedom described under 'Results'. The default convergence criteria were used for the energy minimisations; however, 'tight' convergence criteria were requested for all SCF steps. Since the catalytic site is

Keywords: Histone deacetylase; Enzyme catalysis; Density functional theory; Protonation state.
* Corresponding author. Tel.: +32 2 629 3300; fax: +32 2 629 3304; e-mail: kenno.vanommeslaeghe@vub.ac.be

0968-0896/$ - see front matter © 2005 Elsevier Ltd. All rights reserved.
doi:10.1016/j.bmc.2005.04.001

buried at the bottom of a narrow hydrophobic pocket, no solvent model was included in the calculations on this system. However, for the calculations on a free water molecule or hydroxide ion, the SCIPCM[21] solvent model was used. In this case, single centre surface integration has been selected instead of the default multicentre method, using an equally spaced Lebedev grid with 974 integration points. As recommended by Gaussian, inc., SCIPCM calculations were performed with Gaussian 94.

2.2. Calculation of BSSE corrected energy of interaction

All interaction energies were calculated using the counterpoise method for correcting the basis set superposition error (BSSE).[22] For interactions of the active site with a hydroxide ion or water molecule, Gaussian's built-in counterpoise command was used, after which the minimum energies of the active site and the solvated ligand in their respective protonation states were subtracted to account for the conformational change and desolvation on binding. For proton affinities, usage of the built-in counterpoise command was not possible due to the failure of the program in recognising a single proton and assigning its corresponding energy of zero, so the counterpoise correction was performed by calculating the desired energetic contributions separately, again taking into account the conformational change, and, in the case of the hydroxide ion, the solvation.

3. Results

3.1. Catalytic site model

To the HDLP/TSA complex obtained from the Brookhaven Protein Data Bank[23] (entry code 1C3R, resolution: 2.1 Å), hydrogen atoms were added, and their positions were optimised using the ESFF force field[24] as implemented in the Insight II software.[25] The resulting geometry was used as a starting point for the generation of the catalytic site model containing a total number of 103 atoms, shown in Figure 1. This model comprises the catalytically important zinc ion, together with the side chains of its coordinating residues Asp 168, His 170 and Asp 258. The main chain between Asp 168 and His 170 was retained, because the hydrogen bonds from aspartates 168 and 258 to the two amide NH atoms in this backbone segment will likely influence the electrostatic interactions upon coordination. The phenolic side chain of Tyr 297 was added because its position in the active site suggest that it plays an important role in catalysis, which is supported by mutagenesis experiments.[12] Also, the side chains of the two His–Asp charge relay systems, His 131–Asp 168 and His 132–Asp 173, were included, because of their alleged role in catalysis. Finally, the C_α atom of Asp 173 was retained, together with the carbonyl group of Asp 173 and the NH group of Gly 174, because this NH is hydrogen bonded to Asp 173, which may directly influence the basicity of the whole charge relay system. We consider this model sufficiently extended for a pure quantum chemical approach, as the closest polar centre that was not included in the model is the amide nitrogen of Gly 295, located at a distance of 4.6 Å from the catalytic Zn^{2+} ion, and the closest charged group is a sodium or potassium ion at 7.4 Å. Moreover, these groups, as well as all other polar moieties surrounding the catalytic side model, are shielded from the catalytic Zn^{2+} ion by bulk protein, so that they are not likely to interfere directly with catalysis. On this model system, a DFT/B3LYP study was conducted, using the 6-31G* basis set as a starting point for all atoms. Diffuse functions were added to all non-hydrogen atoms involved in binding or in proton transfers (the catalytic zinc ion, the phenolic oxygen atom of Tyr 297, the four nitrogen atoms of His 131 and His 132 and the four side-chain oxygen atoms of Asp 166 and Asp 173) and to the oxygen atom of the active site-bound hydroxide ion or water molecule.

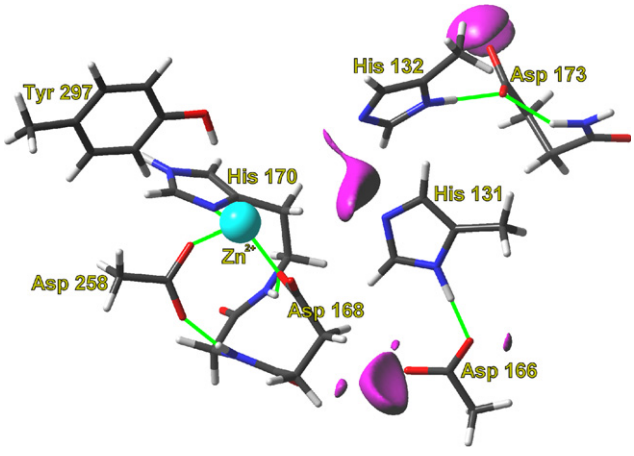

Figure 1. Empty unprotonated active site of HDLP. The electrostatic isopotential surface at −0.284 a.u. is shown in magenta. Non-covalent bonds are marked in green.

In all subsequent geometry optimisations, the heavy atoms from the X-ray structure were kept fixed because a full minimisation on the catalytic site would lead to large structural deviations due to the lack of the rest of the protein, which is needed to keep the active site in shape. The OH hydrogen atom of Tyr 297 was allowed to move, as well as any ligand present in the active site and any protons interacting with the imidazole nitrogen atoms of His 131 and His 132. All other hydrogen atoms were kept fixed, because they are bound to the heavy atoms in the X-ray structure. Following the minimisations, interaction energies between the active site and the ligand were determined, as well as proton affinities, using the procedure discussed under 'computational details'.

3.2. Force relaxations of the empty active site

Both His–Asp dyads in the active site can either be or not be protonated at N^τ, yielding four different combinations for the protonation state of the active site. Additionally, for a protonated His–Asp system, the N^π proton of the histidine can either remain bound to N^π, or be transferred onto the aspartate residue, or alternatively exist in an intermediary situation.[26] After minimisation of the two extreme starting configurations, the latter turned out to be the case for the His 131–Asp 166 pair, whilst two distinct configurations were found

Table 1. Results of geometry optimisations

Protonation state at N^{τ}(X = protonated)		Ligand	Proton affinity		ΔE of proton transfer[a]	Ligand binding energy
His 131	His 132		His 131 N^{τ}	His 132 N^{τ}		
		None				
X		None	−382.9			
	X	None		−359.8	−1.4	
X	X	None	−324.2	−301.2	N/A[b]	
		OH^-				36.8
X		OH^-	−433.1			−13.3
	X	OH^-		−409.6	5.4	−13.3
X	X	OH^-	−373.4	−349.8	−1.9	−63.6
		H_2O				−44.7

All energies are reported in kilocalories per mole.

[a] ΔE of proton transfer from His 132 N^{π} to Asp 173. Out of the two consequent protonation states, the one with the lowest energy is described in the table.

[b] Not calculated, but can be inferred from the other results to be negative and lower than -1.4 kcal mol^{-1}.

for His 132–Asp 173. These findings indicate the absence of an energetic barrier to the displacement of the N^{π} proton in the former case and the presence of such a barrier in the latter case.

Consequently, both configurations were considered for all species protonated on His 132 N^{τ}, while for the species protonated on His 131 N^{τ}, an intermediate situation was used as a starting structure. This resulted in a total of six force relaxations on the empty active site.

Subsequently, proton affinities were calculated for the N^{τ} atoms of His 131 or His 132 (Table 1).

3.3. Force relaxations of a water molecule in the active site

Preliminary calculations indicated that a water molecule coordinating the catalytic zinc ion is likely to be deprotonated by His 131.[27] To verify this hypothesis, the energy minimum of a water molecule in the unprotonated active site was compared to the minimum of a hydroxide ion in the active site, protonated at His 131. This resulted in an energy difference of 20.2 kcal mol^{-1}[†] in favour of the latter, confirming the deprotonation of water when bound to HDLP. Also, the resulting hydroxide ion accepts a hydrogen bond from Tyr 297 in the final geometry. Subsequently, minimisations of the active site containing a OH^- ion were performed, taking the same six protonation states into consideration as for the empty active site. Then, proton affinities were again calculated, and additionally, the binding energy of the hydroxide ion was obtained (Table 1).

4. Discussion

4.1. The His–Asp charge relay systems

Already from geometrical considerations, it is apparent that both His–Asp dyads are different in structure and function. More specifically, the distance between His 131 N^{π} and the nearest carboxylate oxygen of Asp 166 is 2.5 Å and the imidazole ring is in plane with the carboxylate group, resembling the short, strong hydrogen bond in the 'basic' His–Asp pair in serine proteases.[28] In contrast, in the His 132–Asp 173 dyad, the distance is 2.8 Å and both groups are in completely different planes from one another, which makes it more similar to the 'acidic' His–Asp pair of ribonucleases,[29] in which a 'weak' hydrogen bond is present.[30] These differences are reflected in an energetic barrier to proton transfer in the His 131–Asp 166 pair that is absent in the His 132–Asp 173 pair. Moreover, the proton affinities of the His residues differ by 23.1 kcal mol^{-1}, which implies that, while His 131 will preferably be protonated by an active site-bound water molecule, this is not the case for His 132. This suggests that in the catalytic mechanism, His 131 could function as 'general base' and His 132 as 'general acid', as expected from the geometry.

Less trivial is that the charge separation induced by the protonation of one of the His–Asp dyads strongly disfavours the protonation of the other. When comparing the proton affinity of one of the His residues in the empty, unprotonated active site to the proton affinity of the same His residue when the active site is protonated on the other His residue, the magnitude of this effect amounts in both cases to about 60 kcal mol^{-1}. The latter value may however be an overestimation, since in the complete protein, the effect of the abovementioned charge separation may be partially counteracted by induced polarisation of the surrounding 'bulk protein'. This damping effect is difficult to quantify, given our computational limits. However, to establish a lower limit for the coupling energy between the two His–Asp pairs, the proton affinity of one His residue in the empty and otherwise unprotonated active site can be compared to the proton affinity of the same residue when the active site is protonated on the other histidine and an OH^- ion is present in the active site, the latter functioning as a crude and exaggerated mimic of the polarisation of the 'bulk protein'. This difference is about 10 kcal mol^{-1}, so that the actual coupling energy of the two His–Asp pairs can be expected to lie between 10 and 60 kcal mol^{-1}, clearly indicating that the negative

[†] Non-BSSE corrected; BSSE corrected value: 18.7 kcal mol^{-1}. 1 cal = 4.184 J.

coupling between the protonation of the two His–Asp dyads will have a significant impact on their functioning.

4.2. Electrostatic potential

In order to gain additional insight into the functioning of the active site as a whole, the electrostatic potential of the empty, unprotonated active site was investigated. As expected, the minimum near His 131 N^{τ} (−0.316 a.u.) is deeper than the minimum near His 132 N^{τ} (−0.287 a.u.) Also, the isopotential surface at −0.284 a.u. (Fig. 1) shows a connection between the minima of His 131 and His 132, which disappears in the isopotential surface at −0.285 a.u. (not shown). Hence, the saddle point in the electrostatic potential must be situated between these two values, and consequently, the activation energy of the proton transfer from $HisH^{+}$ 132 to His 131 can roughly be estimated at −0.284 a.u. + 0.287 a.u. = 0.003 a.u. or 2 kcal mol^{-1}, suggesting that a proton transfer from His 132 to His 131 will readily occur at biologically relevant temperatures.

4.3. Protonation state of the empty active site

As demonstrated by theoretical[31] as well as experimental[32] studies, the catalytic Zn^{2+} ion will significantly increase its ligand's acidity. Moreover, the acidity of an active site-bound water molecule may be further increased by accepting a hydrogen bond from either His 131 or Tyr 297. However, the magnitude of these effects cannot be inferred from our calculations, because the net charge of our active site model makes comparison of proton affinities in the active site with 'free' proton affinities impossible.

Still, it is possible to determine the native state of the protein, which yields valuable information about its catalytic mechanism. From the strongly negative energy for transferring a proton from an active site-bound water molecule to His 131 (−18.7 kcal mol^{-1}), it can be concluded that the latter will be protonated in the native state of the enzyme. Additionally, the large binding energy of the resulting hydroxide ion in the protonated active site (−13.3 kcal mol^{-1}) suggests that this ion will remain bound in the active site, in analogy with the carbonic anhydrase class of zinc enzymes.[32] Also, the large difference in proton affinity between His 131 and His 132 (+23.4 kcal mol^{-1} in the presence of an OH^{-} ion) excludes a consecutive proton transfer from the former to the latter. Consequently, the source of a proton for His 132 could only be a second water molecule.

When, as a starting point, the protonation of His 132 by a single active site-bound water molecule is considered:

$$\begin{aligned}\Delta E &= -\Delta E_{\text{bind}}(\text{H}_2\text{O-HDLP}^0) - \Delta E_{\text{prot}}(\text{OH}^-) \\ &\quad + \Delta E_{\text{prot}}(\text{His 132}) + \Delta E_{\text{bind}}(\text{OH}^-\text{-HDLP-H 132}^+) \\ &= (44.7 + 332.9 - 359.8 - 13.3)\ \text{kcal mol}^{-1} \\ &= +4.5\ \text{kcal mol}^{-1}\end{aligned}$$

the results suggest moderately unfavourable energetics. However, the effects of the preceding protonation of His 131 by a zinc-bound water molecule are neglected in this approach. More precisely, the presence of a Zn^{2+}-bound OH^{-} ion will sterically and electrostatically disfavour the formation of a second hydroxide ion, and, as mentioned above, the protonated form of His 131 will disfavour the subsequent protonation of His 132. The influence of the former effect is difficult to infer from our results but can be expected to be very significant, and, as argued above, the magnitude of the latter effect amounts to 10–60 kcal mol^{-1}, out of which can be concluded that the protonation of His 132 is unfavourable

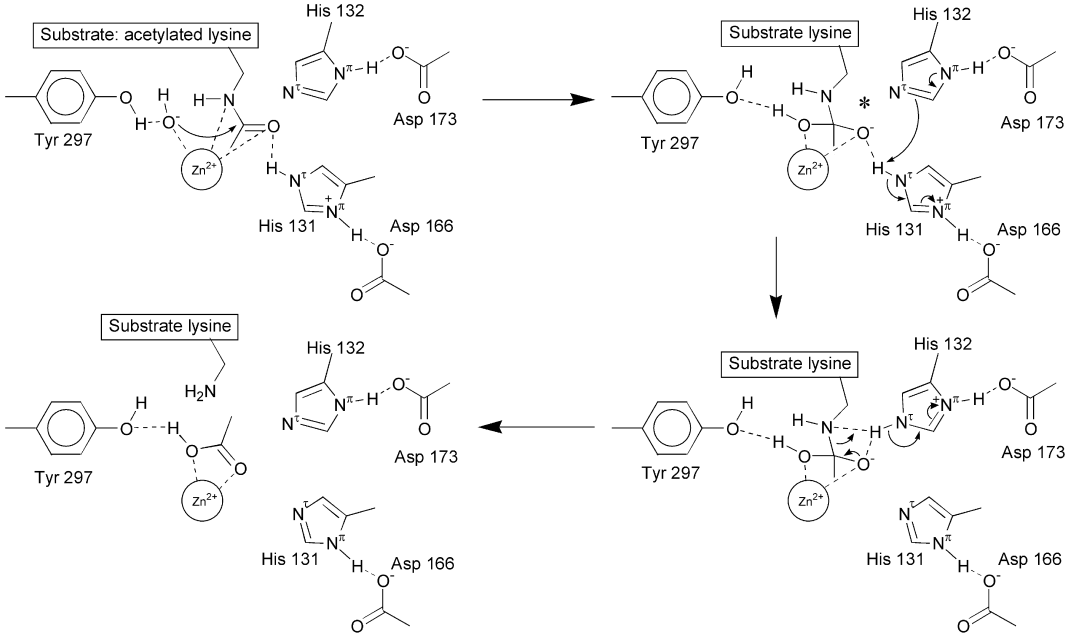

Scheme 1. Tentative catalytic mechanism for HDAC.

by at least 14 kcal mol^{-1}, and probably by much more. Thus, it is reasonable to assume that the starting situation for the catalytic mechanism will be an active site, protonated at His 131 but not at His 132, with a hydroxide ion coordinating the catalytic zinc ion, as shown in Scheme 1.

4.4. Catalytic mechanism

In summary, the most important results of the present work are: (a) His 131 has pronounced basic characteristics, whilst His 132 is more acidic; (b) simultaneous protonation of His 131 and His 132 is unlikely because protonation of the one strongly inhibits protonation of the other; (c) a low potential channel between His 131 N^{τ} and His 132 N^{τ} should facilitate proton transfer; (d) the native state of the active site was identified. Based on these findings and starting from the abovementioned native state, we propose the following catalytic mechanism (Scheme 1). Upon binding of an acetylated lysine side chain, the zinc-bound hydroxide ion would attack the amide carbon, in analogy with the mechanism of carbonic anhydrase.[32] The result is a tetrahedral transition state, in which an excess of negative charge is expected between His 132 N^{τ} and the amide nitrogen, indicated by the symbol * in Scheme 1. This energetically unfavourable situation could be resolved by transferring His 131's N^{τ} proton to His 132, via the low potential channel that exists between these two residues. From there, taking into account the higher acidity of His 132, protonation of the amide nitrogen is evident, resulting in the cleavage of the amide bond. Finally, after a proton transfer from acetic acid to the histone's lysine and the subsequent release of the products (not shown in the scheme), a new water molecule may bind the Zn^{2+} ion and protonate the basic His 131 to complete the catalytic cycle.

4.5. Similarities between HDLP and hHDAC8

The significance of the present results strongly depends on the premise that HDLP is a good model for human HDACs in general and the class I HDACs in particular.[11] Since HDAC8, of which a TSA-bound X-ray structure was recently published (PDB[23] entry code 1T64, resolution: 1.9 Å),[13] belongs to this class, it is a relevant point of reference in this respect. The RMSD after overlap of all 56 heavy atoms in our catalytic site model with the corresponding atoms in HDAC8 is 0.41 Å (Fig. 2).

Despite the high similarity revealed by this picture, two problems remain to be addressed: a shift in atomic positions of 0.4 Å can disrupt the short, strong hydrogen bond detected in this paper, as well as the low potential channel. However, a closer examination learns that the measured RMSD is mainly the result of a repositioning of the different catalytic motifs in the site. Consequently, the RMSD between the heavy atoms of the indole ring and the carboxylate group of the His 131–Asp 166 dyad in our model and the corresponding dyad in HDAC8 is only 0.12 Å, and the distance between the N^{π} atom of the His residue and the nearest carboxylate oxygen of the Asp residue in this dyad is even 0.05 Å shorter in

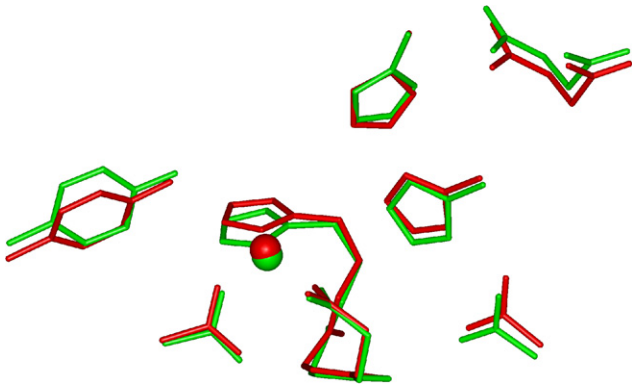

Figure 2. Overlap between the catalytic sites of HDLP (green) and hHDAC8 (red).

HDAC8, confirming the presence of a short, strong hydrogen bond. Measured analogously, the RMSD for the His 132–Asp173 dyad is 0.11 Å and the His–Asp distance in HDAC8 is 2.71 Å, which is 0.12 Å shorter than in HDLP, but still within the limits for an 'weak' hydrogen bond.[28] Thus, our conclusions regarding the His–Asp hydrogen bonds and the acid-base properties of the catalytic histidine residues remain unchanged. As for the low potential channel, the distance between the N^{τ} atoms of both histidines is 0.33 Å shorter in HDAC8, which makes the presence of this channel even more likely. Overall, it can be concluded that, if the proposed mechanism is correct for HDLP, it probably also holds for HDAC8 and the other class I HDACs.

5. Conclusions

The catalytic site of HDLP was thoroughly investigated at B3LYP/6-31G* level. In the His 132–Asp 173 charge relay system, an energetic barrier for the displacement of the N^{π} proton was found to be present, while in the His 131–Asp 166 pair, no such barrier was shown to exist. The difference in proton affinity between the two His–Asp charge relay systems was determined, and a negative coupling between the protonation of the two His–Asp systems was observed and quantified at more than 10 kcal mol^{-1}. An electrostatic potential was generated for the empty unprotonated active site, and a low potential channel was observed between the minima near the N^{τ} atoms of His 131 and His 132. All combined, these results strongly indicate that HDAC, in its native state, is protonated at His 131 but not at His 132, and contains a hydroxide ion that is bound to the active site zinc ion with a binding energy of -13 kcal mol^{-1}. Based on these findings, a catalytic mechanism that differs from other metalloproteases was suggested. This mechanism also differs from the previous proposal by Finnin et al.,[12] in the native protonation state of the His–Asp dyads, and in the deprotonation of water as a distinct step in the mechanism. As the geometric similarity between HDLP and a human class I HDAC is strong enough to assume conservation of this mechanism, our findings may have implications for the kinetics of this pharmaceutically highly relevant class of enzymes.

Acknowledgements

K. Vanommeslaeghe is a Research Assistant of the Fund for Scientific Research Flanders (Belgium) (FWO-Vlaanderen). P. Geerlings also thanks the FWO-Vlaanderen for continuous support of his research group. The authors are also grateful to C. Van Alsenoy of the University of Antwerp for his support in the initial stage of this work.

Supplementary data

Supplementary data associated with this article can be found, in the online version at doi:10.1016/j.bmc.2005.04.001.

References and notes

1. McLaughlin, F.; Finn, P.; La Thangue, N. B. *Drug Discov. Today* **2003**, *8*, 793–802.
2. Warrener, R.; Beamish, H.; Burgess, A.; Waterhouse, N. J.; Giles, N.; Fairlie, D.; Gabrielli, B. *FASEB J.* **2003**, *17*, 1550–1552.
3. Rombouts, K.; Niki, T.; Greenwel, P.; Vandermonde, A.; Wielant, A.; Hellemans, K.; De Bleser, P.; Yoshida, M.; Schuppan, D.; Rojkind, M.; Geerts, A. *Exp. Cell Res.* **2002**, *278*, 184–197.
4. Niki, T.; Rombouts, K.; De Bleser, P.; De Smet, K.; Rogiers, V.; Schuppan, D.; Yoshida, M.; Gabbiani, G.; Geerts, A. *Hepatology* **1999**, *29*, 858–867.
5. Papeleu, P.; Loyer, P.; Vanhaecke, T.; Elaut, G.; Geerts, A.; Guguen-Guillouzo, C.; Rogiers, V. *J. Hepatol.* **2003**, *39*, 374–382.
6. Mishra, N.; Brown, D. R.; Olorenshaw, I. M.; Kammer, G. M. *Proc. Natl. Acad. Sci. U.S.A.* **2001**, *98*, 2628–2633.
7. Leoni, F.; Zaliani, A.; Bertolini, G.; Porro, G.; Pagani, P.; Pozzi, P.; Dona, G.; Fossati, G.; Sozzani, S.; Azam, T.; Bufler, P.; Fantuzzi, G.; Goncharov, I.; Kim, S.-H.; Pomerantz, B. J.; Reznikov, L. L.; Siegmund, B.; Dinarello, C. A.; Mascagni, P. *Proc. Natl. Acad. Sci. U.S.A.* **2002**, *99*, 2995–3000.
8. McCampbell, A.; Taye, A. A.; Whitty, L.; Penney, E.; Steffan, J. S.; Fischbeck, K. H. *Proc. Natl. Acad. Sci. U.S.A.* **2001**, *98*, 15179–15184.
9. Steffan, J. S.; Joan, S.; Bodal, L.; Pallos, J.; Poelman, M.; McCampbell, A.; Apostol, B.; Kazantsev, A.; Schmidt, E.; Zhu, Y.-Z.; Greenwald, M.; Kurokawa, R.; Housman, D. E.; Jackson, G. R.; Marsh, J. L.; Thompson, L. M. *Nature* **2001**, *413*, 739–743.
10. Zhang, Y.; Li, N.; Caron, C.; Matthias, G.; Hess, D.; Khochbin, S.; Matthias, P. *EMBO J.* **2003**, *22*, 1168–1179.
11. De Ruijter, A. J. M.; Van Gennip, A. H.; Caron, H. N.; Kemp, S.; Van Kuilenburg, A. B. P. *Biochem. J.* **2003**, *370*, 737–749.
12. Finnin, M. S.; Donigian, J. R.; Cohen, A.; Richon, V. M.; Rifkind, R. A.; Marks, P. A.; Breslow, R.; Pavletich, N. P. *Nature* **1999**, *401*, 188–193.
13. Somoza, J. R.; Skene, R. J.; Katz, B. A.; Mol, C.; Ho, J. D.; Jennings, A. J.; Luong, C.; Arvai, A.; Buggy, J. J.; Chi, E.; Tang, J.; Sang, B.-C.; Verner, E.; Wynands, R.; Leahy, E. M.; Dougan, D. R.; Snell, G.; Navre, M.; Knuth, M. W.; Swanson, R. V.; Mcree, D. E.; Tari, L. W. *Structure* **2004**, *12*, 1325–1334.
14. Vannini, A.; Volpari, C.; Filocamo, G.; Casavola, E. C.; Brunetti, M.; Renzoni, D.; Chakravarty, P.; Paolini, C.; De Francesco, R.; Gallinari, P.; Steinkühler, C.; Di Marco, S. *Proc. Natl. Acad. Sci. U.S.A.* **2004**, *101*, 15064–15069.
15. Siegbahn, P. E. M.; Blomberg, M. R. A. *Chem. Rev.* **2000**, *100*, 421–437.
16. Ban, F.; Rankin, K. N.; Gauld, J. W.; Boyd, R. J. *Theor. Chem. Acc.* **2002**, *108*, 1–11.
17. Mignon, P.; Steyaert, J.; Loris, R.; Geerlings, P.; Loverix, S. *J. Biol. Chem.* **2002**, *277*, 36770–36774.
18. Versées, W.; Loverix, S.; Vandemeulebroucke, A.; Geerlings, P.; Steyaert, J. J. *Mol. Biol.* **2004**, *338*, 1–6.
19. Roos, G.; Messens, J.; Loverix, S.; Wyns, L.; Geerlings, P. *J. Phys. Chem. B* **2004**, *108*, 17216–17225.
20. Frisch, M. J.; Trucks, G. W.; Schlegel, H. B.; Scuseria, G. E.; Robb, M. A.; Cheeseman, J. R.; Montgomery, J. A., Jr.; Vreven, T.; Kudin, K. N.; Burant, J. C.; Millam, J. M.; Iyengar, S. S.; Tomasi, J.; Barone, V.; Mennucci, B.; Cossi, M.; Scalmani, G.; Rega, N.; Petersson, G. A.; Nakatsuji, H.; Hada, M.; Ehara, M.; Toyota, K.; Fukuda, R.; Hasegawa, J.; Ishida, M.; Nakajima, T.; Honda, Y.; Kitao, O.; Nakai, H.; Klene, M.; Li, X.; Knox, J. E.; Hratchian, H. P.; Cross, J. B.; Adamo, C.; Jaramillo, J.; Gomperts, R.; Stratmann, R. E.; Yazyev, O.; Austin, A. J.; Cammi, R.; Pomelli, C.; Ochterski, J. W.; Ayala, P. Y.; Morokuma, K.; Voth, G. A.; Salvador, P.; Dannenberg, J. J.; Zakrzewski, V. G.; Dapprich, S.; Daniels, A. D.; Strain, M. C.; Farkas, O.; Malick, D. K.; Rabuck, A. D.; Raghavachari, K.; Foresman, J. B.; Ortiz, J. V.; Cui, Q.; Baboul, A. G.; Clifford, S.; Cioslowski, J.; Stefanov, B. B.; Liu, G.; Liashenko, A.; Piskorz, P.; Komaromi, I.; Martin, R. L.; Fox, D. J.; Keith, T.; Al-Laham, M. A.; Peng, C. Y.; Nanayakkara, A.; Challacombe, M.; Gill, P. M. W.; Johnson, B.; Chen, W.; Wong, M. W.; Gonzalez, C.; Pople, J. A. *Gaussian 03, Revision B.03*; Gaussian: Pittsburgh, PA, 2003.
21. Foresman, J. B.; Keith, T. A.; Wiberg, K. B.; Snoonian, J.; Frisch, M. J. *J. Phys. Chem.* **1996**, *100*, 16098–16104.
22. Boys, S. F.; Bernardi, F. *Mol. Phys.* **1970**, *19*, 553–566; Van Duijneveldt, F. B.; Van Duijneveldt-Van De Rijdt, J. G. C. M.; Van Lenthe, J. H. *Chem. Rev.* **1994**, *94*, 1873–1885.
23. Berman, H. M.; Westbrook, J.; Feng, Z.; Gilliland, G.; Bhat, T. N.; Weissig, H.; Shindyalov, I. N.; Bourne, P. E. *Nucl. Acids Res.* **2000**, *28*, 235–242.
24. Despite the fact that ESFF is developed for application on anorganic and organometallic molecules, it also is able to generate acceptable results, similar to CVFF, on organic compounds; see: Martins, J. C.; Willem, R.; Biesemans, M. *J. Chem. Soc., Perkin Trans. 2* **1999**, 1513–1520.
25. *Insight II version 98*, Accelrys Inc. (Formerly MSI).
26. Depending on the source, this phenomenon is called 'single well HB', 'strong ionic asymmetric one-well HB', 'deep well HB', 'short, strong HB', 'catalytic HB', etc. Also, it is often inaccurately called 'Low-Barrier HB'. In this article, we will use the term 'short, strong HB', as it seems to be the most broadly accepted. A discussion of the different classes of biochemically relevant hydrogen bonds can be found in: Cleland, W. W. *Arch. Biochem. Biophys.* **2000**, *382*, 1–5.
27. Vanommeslaeghe, K.; Van Alsenoy, C.; De Proft, F.; Martins, J. C.; Tourwé, D.; Geerlings, P. *Org. Biomol. Chem.* **2003**, *1*, 2951–2957.
28. Frey, P. A. *J. Phys. Org. Chem.* **2004**, *17*, 511–520.
29. Wlodawer, A.; Svensson, L. A.; Sjolin, L.; Gilliland, G. L. *Biochemistry* **1988**, *27*, 2705–2717.
30. Quirk, D. J.; Raines, R. T. *Biophys. J.* **1999**, *76*, 1571–1579.
31. Cross, J. B.; Duca, J. S.; Kaminski, J. J.; Madison, V. S. *J. Am. Chem. Soc.* **2002**, *124*, 11004–11007.
32. Woolley, P. *Nature* **1975**, *258*, 677–682.